Journal of Applied Polymer Science

Effects of Nano-TiO_2 on the Properties and Structures of Starch/Poly(ε-Caprolactone) Composites

Peng Fei,[1,2] Yongjun Shi,[1,2] Man Zhou,[1,2] Jie Cai,[1,2] Shangwen Tang,[1,2,3] Hanguo Xiong[1,2]

[1]College of Food Science and Technology, Huazhong Agricultural University, Wuhan 430070, China

[2]Research Institute of comprehensive utilization of Biomaterials, Huazhong Agricultural University, Wuhan 430070, China

[3]School of Chemical Engineering and Food Science, Hubei University of Arts and Science, Xiangyang 441053, China

Correspondence to: H. Xiong (E-mail: xionghanguo@163.com)

ABSTRACT: Poor physical properties resulting from low interfacial interactions between hydrophilic biopolymers and hydrophobic thermoplastic matrices have been one of the biggest obstacles in preparing quality biomass materials. This study concentrates on the effects of nano-TiO_2 on the properties and structure of starch/poly (ε-caprolactone) (PCL) composites. The molecular and crystal structures of the composites were characterized by using Fourier transform infrared spectroscopy, differential scanning calorimeter (DSC), X-ray diffraction (XRD), and field emission scanning electron microscope. The results indicated that an interpenetrating network structure formed by adding nano-TiO_2 into starch/PCL composites. The DSC and XRD analysis indicated that the crystallinity degree and the crystallization rate of the composites reduced, whereas the crystal form and crystal size were unchanged. The results also showed that the mechanical properties and water resistance of the composites were improved significantly with the addition of nano-TiO_2, whereas their transparency decreased. © 2013 Wiley Periodicals, Inc. J. Appl. Polym. Sci. 130: 4129–4136, 2013

KEYWORDS: composites; properties and characterization; structure-property relations; biomaterials

Received 6 March 2013; accepted 23 June 2013; Published online 10 July 2013

DOI: 10.1002/app.39695

INTRODUCTION

Biomass materials which applied to storage compartments, cooler lining, labware consumables, office storage articles, car body panels, food containers, and so on have attracted worldwide attentions during the past decades. Such attention is not only because of the environmental concerns, but also of the necessity of providing a high-performance, multi-functional product at a low-cost.[1–3] In the past decades, various attempts have been focused on blending plastic materials with cheap and biodegradable natural biopolymers with desired properties. Starch, as an abundant renewable polysaccharide with better biodegradability, is one of the most potential materials for biodegradable plastics production.[4–7] Except for starch, which is a natural biodegradable biopolymer, there is another promising class of synthetic biodegradable materials, such as poly(ε-caprolactone) (PCL),[8] poly(lactic acid) (PLA), poly(hydroxy butyrate) (PHB), poly(glycolic acid) (PGA),[9] polybutylene succinate (PBS), polybutylene succinate adipate copolymer, and polyethylene succinate.[10] Among them, PCL, as a linear, hydrophobic, and semicrystalline polyester with a very high flexibility, is particularly a promising polymer.[11] It is relatively stable against abiotic hydrolysis, but it is easily degraded and utilized as carbon source by various microorganisms,[12,13] because the polar ester group among PCL molecular chains could be easily decomposed by microbiology or enzyme with the final product of CO_2 and H_2O. PCL has been reported to be biodegradable in various environments, e.g., in pure fungal cultures,[14] compost,[15] active sludge,[16] and soil. Moreover, the ultimate tensile strength and the elongation at the break of PCL films have been reported to be around 33 MPa and 1100%, respectively.[17] Its physical properties and commercial availability make it very attractive, not only as a substitute of nonbiodegradable polymers for commodity applications, but also for specific applications in medicine and in agricultural areas.[18]

The main limit of starch/PCL composites is the weak adhesion between the hydrophilic polysaccharides and the hydrophobic polyester matrix, which may lead to the poor physical properties of the composites. Many efforts have been devoted to overcome this situation involving the grafting of compounds onto the polymers by using various coupling agents or bonding agents or the pretreatment of polymers with suitable chemicals.[19] According to the previous literature,[20] maleic anhydride (MA) was grafted onto PCL and the MA noticeably improved the mechanical properties of PCL/starch composites. Chen et al.[21] used the PLLA grafted starch copolymer as compatibilizer to improve the interfacial adhesion between PCL matrix and starch.

The addition of small quantities of inorganic materials dispersed at a nanometric level has been proven as one of the most promising strategies to improve the physical and mechanical properties of polymers and blends. Vertuccio et al.[22] studied the reinforcement of nanoclay with PCL/starch blends, and they found that the addition of inorganic materials dispersed at a nanometric level was an effective method to overcome the weak adhesion between starch and thermoplastic. Thipmanee et al.[23] used zeolite 5A as an inorganic phase to reinforced PCL/starch blends, and they reported that zeolite 5A could improve the physical properties of the composites. Anatase nano-TiO_2, which is an inorganic nanoparticle with large specific surface area and high surface energy, has been widely employed in research and development of solar cell,[24] sewage disposal,[25] antibacterial materials,[26] and self-cleaning materials[27] because of its high photocatalytic activity. In addition to these structures, several -OH groups and dangling bonds can be adsorbed on the surface of nano-TiO_2, which may remarkably affect the physical properties of natural polymers/thermoplastic composites. However, relevant studies have seldom been reported.

In this study, starch/PCL composites were prepared from corn starch, PCL, nano-TiO_2, and glycerine. The effect of the nano-TiO_2 contents on the physical properties and the structure of the composites were investigated.

EXPERIMENTAL

Material

Corn starch was provided by Huanglong Food of Gongzhuling City (moisture content 11.7%, protein 0.23%, fat 0.075%, ash content 0.08%). PCL ($M_n = 70{,}000$) pellets were acquired from Daicel Chemical Industries, Ltd, Japan. Hydrophilic anatase nano titanium dioxide (nano-TiO_2), with a particle size of 60 nm, was provided by the Nanometer Engineering Center of the People's Republic of China. Glycerine and absolute ethyl alcohol were analytical grade and used as received.

Sample Preparation

Starch (6 g) and glycerin (18 g) were added into JB200-D electromotion stirrer (Shanghai specimen and model factory, China) and stirred at high-speed (>1000 rpm) in a constant temperature at 353 K for 20 min to plasticize the starch. PCL (100 g) was added and stirring for 60 min. Finally, the obtained composite was compression molded at 353 K into 1- and 4-mm thick sheets at a pressure of 25 MPa for 5 min via a hot press R-3202 (Wuhan Qien science & Technology Development, China), and coded as SPN0.

Different amounts of nano-TiO_2 (3.2, 6.4, 9.6, and 12.8 g, respectively) were added into a beaker with corresponding volumes of absolute ethyl alcohol (150, 300, 450, and 600 mL, respectively), and dispersed at 600 W for 30 min by a Ultrasonic Processor FDL-1200 (Nanjing Fandilang Info Technology, China) (intermittent dispersion of pulsing on for 1 s and off for 2 s, with a frequency of 20 kHz and an amplitude of 20 μm). Starch (60 g) and glycerin (18 g) were added and stirred with motor stirrer at high-speed (>1000 rpm) in a constant temperature water bath at 353 K for 20 min. Afterwards, the mixture and PCL (100 g) were added into the prepared TiO_2 solutions, respectively. And then the composite solutions were stirred using a motor stirrer at high-speed (>1000 rpm) at 353 K until the ethyl alcohol was evaporated completely. Finally, the composites were compressed into 1- and 4-mm thick sheets as same as the former. The composites with different nano-TiO_2 contents were coded as SPN1, SPN2, SPN3, and SPN4, respectively.

Characterizations

The surfaces and morphologies of starch/PCL composites were investigated by a Hitachi (Japan) S-4800 field emission scanning electron microscope (FESEM). The surfaces were sputter coated with gold prior to examination. The FT-IR spectra were recorded at a Nicolet (USA) Nexus 470 FT-IR spectrometer. Each spectrum consists of 32 scans taken at 4 cm^{-1} resolution and the wavenumber ranged from 4000 to 400 cm^{-1}. The thermal properties of the composite were performed by using a DSC 200PC (NETZSCH, Germany) under nitrogen atmosphere. The samples of 5–10 mg were encapsulated into aluminum pans and were heated from 273 to 378 K at a rate of 10 K/min, and then the temperature was kept at 378 K for 10 min to erase previous thermal history.[29] Subsequently samples were cooled to 283 K at the rate of 10 K/min to obtain the crystallization curve and kept at this temperature for 10 min; after that, the samples were heated to 378 K at the rate of 10 K/min to obtain the melting curve. X-ray diffraction (XRD) measurements were performed on the sample composites by means of a Rigaku (Japan) D/max-RB X-ray diffractometer, and a CuKα target was used at 40 kV and 50 mA. The diffraction angle ranged from 60° to 5°.

Mechanical Properties

The bending strength and bending modulus of the composites were determined by using a Tianyuan NTY8000 electron tensile tester (Jiangsu Tianyuan Test Equipment, China) according to the Chinese standard method GB/T 9341-2008 (Plastic-Determination of flexural properties). The measurements were carried out at room temperature. Cut the prepared composites (SPN0, SPN1, SPN2, SPN3, and SPN4) into 100 × 50 × 4 mm sheets, with the set of span length (the distance between the two clamps) at 80 mm, a loading rate of 10 mm/min and breaking load of 200 N. The thickness of the samples was measured for 10 times by using a micrometer (Mitutoyo Corp., Code No. 543-551-1, Model ID-F125, Japan).

Water Absorption and Water Solubility

The 100 × 100 × 4 mm dried sheets were weighed (W_0) and immersed in distilled water at room temperature (298 K) for 24 h. Then moisture on the surface of the composite was removed with filter paper, and the weight of the composites was measured (W_e). Then the composites were dried in vacuum again at 313 K for 24 h, and the dried composites were weighed (W_d). The water absorption (W_a) in the composite was calculated using the following equation[28]:

$$W_a = \frac{W_e - W_0}{W_0} \times 100\% \quad (1)$$

The water solubility (W_s) was calculated using the following equation:

$$W_s = \frac{W_0 - W_d}{W_0} \times 100\% \quad (2)$$

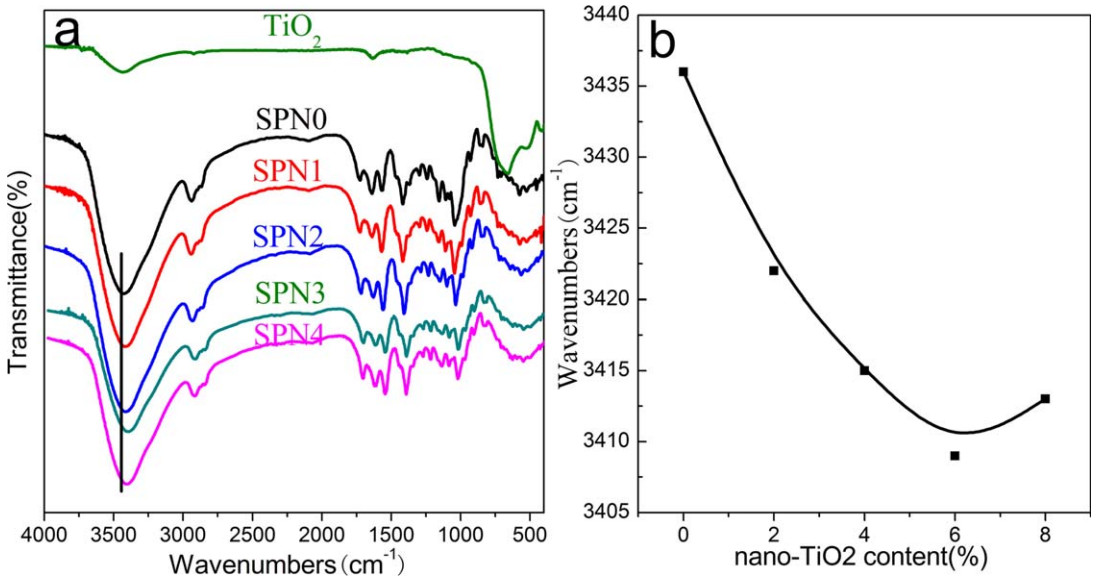

Figure 1. FTIR spectra of nano-TiO_2 and SPN composites: (a) FTIR spectrum of nano-TiO_2 and SPN composites; (b) the O-H stretching of SPN composites; SPN0, SPN1, SPN2, SPN3, SPN4 correspond to increasing nano-TiO_2 contents from 0 to 8 wt %.[Color figure can be viewed in the online issue, which is available at wileyonlinelibrary.com.]

Optical Transparency

The transmittance of the composites (0.15 mm thickness) was measured by using a Shimadzu UV-1700 spectrophotometer (Shimadzu, Kyoto, Japan) in the wavelength range of 450–800 nm.

Statistical Analysis

Experimental data were analyzed statistically by SPSS 17.0, and multiple comparisons methods were accomplished with Duncan's Multiple Range Test ($P \leq 0.05$).

RESULTS AND DISCUSSION

FTIR Analysis

The FTIR spectra of nano-TiO_2 and SPN composites are shown in Figure 1(a). From the spectrum of nano-TiO_2, the absorption peaks at 656, 532, and 412 cm^{-1} were attributed to the characteristic peaks of nano-TiO_2. The peaks at 3435 and 1637 cm^{-1} assigned to the stretching vibration of -OH and bending vibration of Ti-OH respectively,[30] indicating plenty of -OH was on the surface of the nano-TiO_2.

Figure 1(a) also shows the spectra of the SPN composites exhibiting a broad and strong absorption around 3420 cm^{-1} assigned to the characteristic absorption of the stretching vibration of -OH and the hydrogen bonds formed among the -OH groups. The peak for the O-H stretching of the SPN composites is shown in Figure 1(b). The formation of hydrogen bonds reduced the force constant of the participants, thereby resulting in a red shift. Obviously, the absorption band of the -OH shifted to a lower wavenumber with increasing the contents of nano-TiO_2, indicating an increase of hydrogen bonds, because the free -OH on the surface of nano-TiO_2 combined with that of starch and formed intermolecular hydrogen bonds. When the content of nano-TiO_2 reached 8 wt %, the absorption band of -OH shifted to a higher wavenumber, indicating a decrease of the hydrogen bonds. Here, the quantity of free -OH on the surface of starch continually decreased with the increasing amount of nano-TiO_2, leading to the saturation of the reaction between the free -OH of nano-TiO_2 and that of starch. Coupled with increasing the density of nano-TiO_2, the agglomeration of nano-TiO_2 occurred and caused the blue shift.

The formation of hydrogen bonds between nano-TiO_2 and starch/PCL molecules greatly enhanced the cross-linking of the SPN composites. Aside from -OH, large amount of unsaturated dangling bonds were on the surface of nano-TiO_2, because of its small size and high surface energy,[31–34] as seen in Figure 2. TiO_2 is a kind of semiconductor material, a Ti atom was connected to other Ti atoms via bridging oxygen atoms and the total chemical composition was denoted TiO_2. This structure left unpaired electrons (dangling bonds) on surface Ti or O atoms, and the quantity of dangling bonds was proportional to the surface atomic number and inversely proportional to the molecular size of nano-TiO_2. These dangling bonds could form covalent interactions with starch/PCL composites, such as C-O-Ti. Figure 3 shows the FTIR spectra of the composites from 1200 to 850 cm^{-1}. Compared with that of SPN0, the composites contained nano-TiO_2 exhibited an obvious peak at 995 cm^{-1}, attributed to the formation of the C-O-Ti groups. It confirmed that the covalent interactions formed between nano-TiO_2 and starch or between nano-TiO_2 and PCL.

Morphology of the Composites

The morphology of starch/PCL composites was characterized by FESEM (Figure 4). The surface of SPN0 presented a heterogeneous lamellar structure, whereas a clear microporous structure appeared on the surface of the films (SPN1, SPN2, SPN3, SPN4), indicated that a network structure was formed between

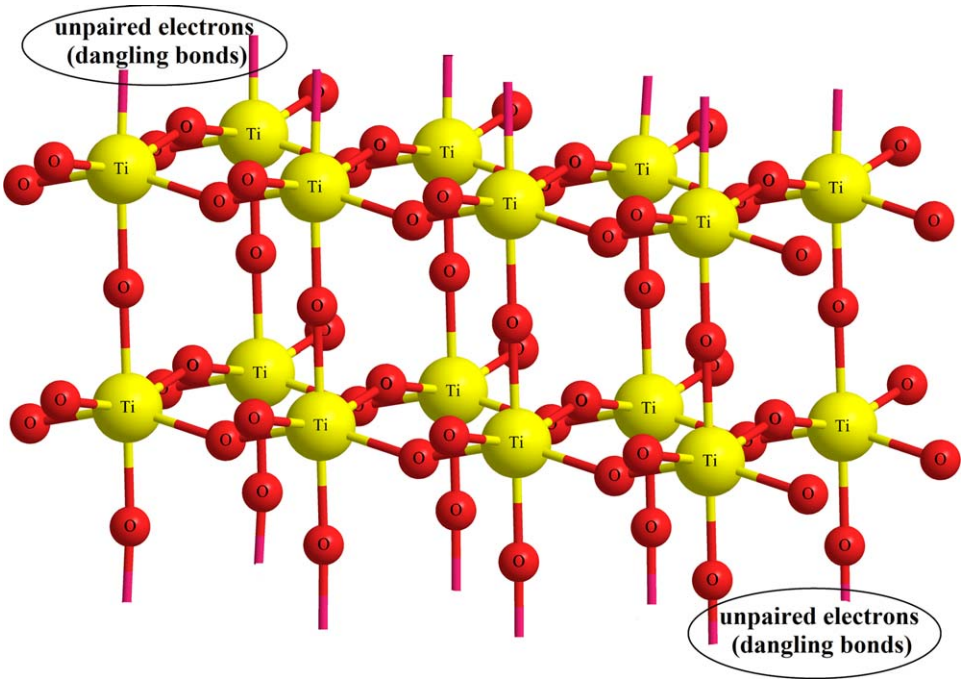

Figure 2. Molecular structure and dangling bonds of nano-TiO_2. [Color figure can be viewed in the online issue, which is available at wileyonlinelibrary.com.]

nano-TiO_2 and starch/PCL. The interactions between nano-TiO_2 and polymer matrix were also performed to fabricate and maintain the 3D-networks among native starch.[35] Besides, the quantity of micropores was proportional to the content of nano-TiO_2, indicated that the network structure was improved continually. However, the quantity of micropores exhibited a decreasing tendency when the content of TiO_2 reached 8 wt %, which verified the agglomeration of the excessive nano-TiO_2.

DSC Analysis

Figure 5 represents the DSC melting curves and crystallinity degree (X_c) of the SPN composites. The crystallinity degree of the PCL component in the composites was determined by the melting peak area using the following equation:

$$X_C = \frac{\Delta H_{\mathrm{m}}}{\varphi \Delta H_m^0} \times 100\% \quad (3)$$

where ΔH_m is the enthalpy of fusion of the sample, ΔH_m^0 is the heat of fusion for 100% crystalline PCL (139.5 J/g)[36], and φ is the weight fraction of PCL in the composites.

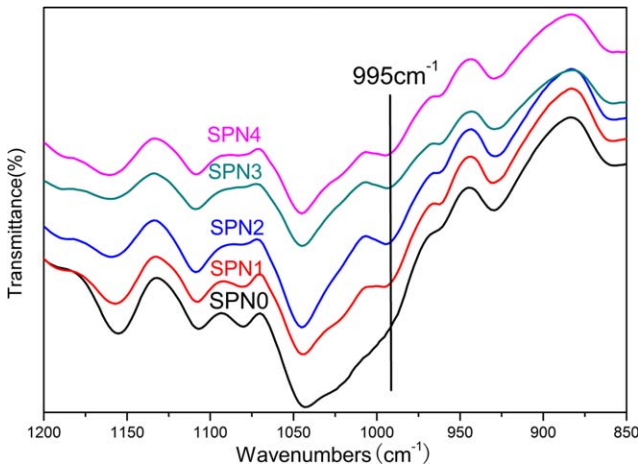

Figure 3. FTIR spectra of SPN composites. [Color figure can be viewed in the online issue, which is available at wileyonlinelibrary.com.]

As shown in the inset (Figure 5), the crystallinity degree was reduced from 73.15% to 59.45% when content of nano-TiO_2 increased from 0 to 6 wt %. It demonstrated that the crystallinity degree decreased with larger amount of crosslinking. Because of its small size, nano-TiO_2 was easily dispersed into the macromolecular chains and formed hydrogen and covalent bonds with starch or PCL. The hydrogen and covalent bonds disturbed the parallel direction of the starch/PCL chains and further restricted the molecular motion and rearrangement. Besides, the addition of nano-TiO_2 could strengthen the rigidity of starch/PCL chains, which also hindered the crystallization of the composites. Based on the above reasons, the crystallinity degree of the composites decreased.

The DSC cooling thermograms and the crystallinity versus time for crystallization of SPN composites during the cooling crystallization process are plotted in Figure 6. The crystallization time of the composites was determined using the following equation:

$$t = \frac{T_0 - T}{\theta} \quad (4)$$

where T_0 is the initial crystallization temperature, T is crystallization temperature, and θ is cooling rate.

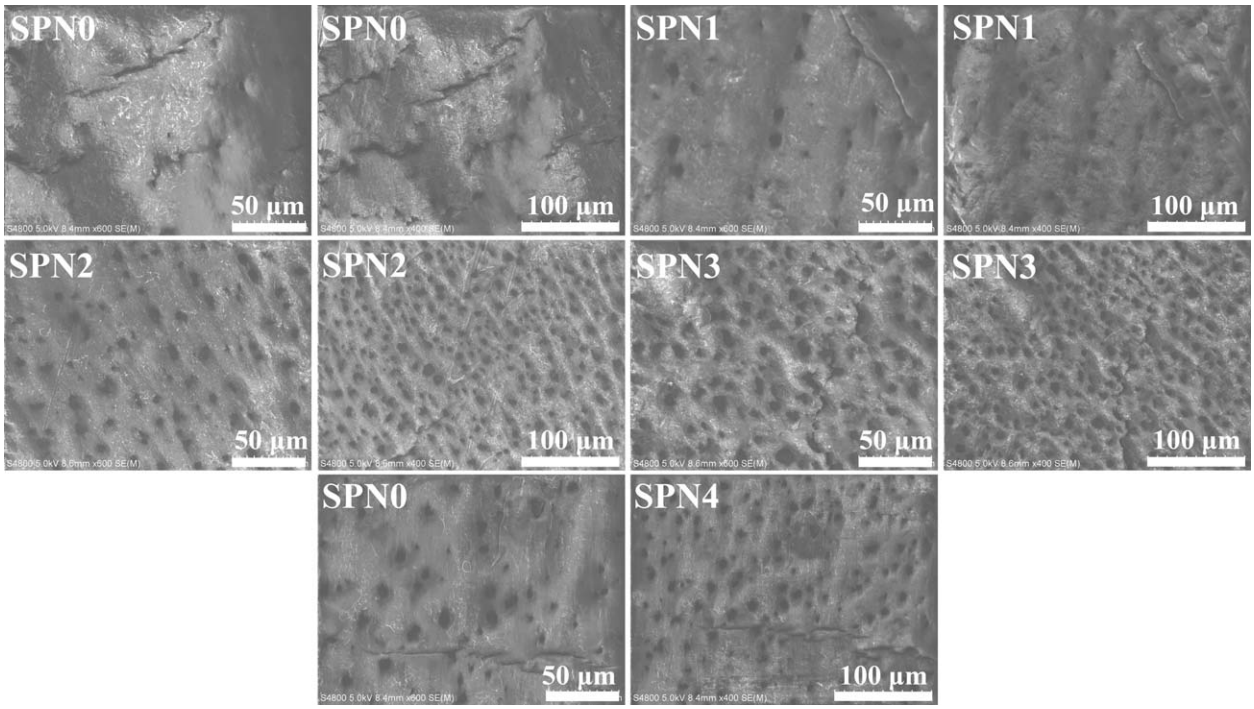

Figure 4. FESEM micrographs of the surfaces of SPN composites.

In Figure 6(b), the crystallization rate and crystallinity degree decreased substantially, and the initial crystallization time was delayed with the increase in nano-TiO_2 content, which was corresponding to the result that the addition of nano-TiO_2 hindered the crystallization of the starch/PCL composites.

XRD Analysis

In Figure 7, the baseline was eliminated and a peak fitting program was used to investigate the crystallinity degree and crystalline form of the samples.[37] There were two main diffraction peaks at $2\theta = 21.87°$ and 24.21°, assigned to the reflections of (110) and (200) planes, respectively. Obviously, by adding nano-TiO_2, the intensities of both the two diffraction peaks were weakened substantially, indicating the destruction of crystalline structure.

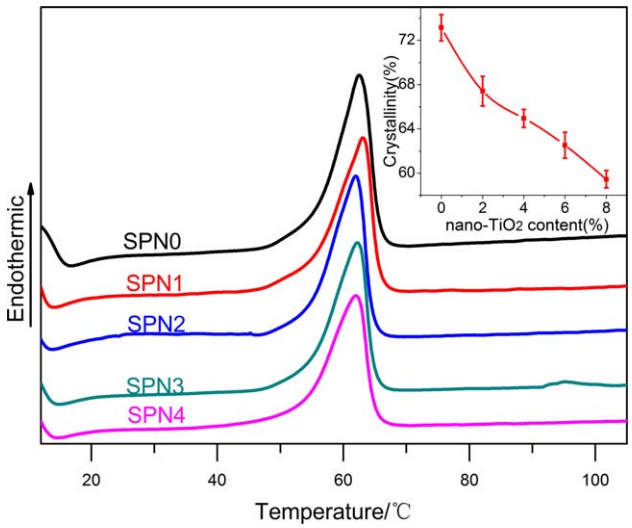

Figure 5. DSC melting curves and the crystallinity degree of SPN composites. The differences of crystallinity degree of SPN composites are significant ($P \leq 0.05$). [Color figure can be viewed in the online issue, which is available at wileyonlinelibrary.com.]

The crystallinity degree of the composites was calculated through the crystalline and noncrystalline areas using the following equation:

$$X_c = \frac{F_c}{F_c + F_a} \times 100\% \quad (5)$$

where F_c is the crystalline area and F_a is the noncrystalline area. The results were shown in the inset (Figure 7), where the crystallinity degree of the composites decreased with an increase in nano-TiO_2. The crystallinity degree of SPN0 was 59.96%, whereas SPN4 possessed the lowest crystallinity degree at 45.89%. The result implied that the variation trend of crystallinity degree corresponded to the results of DSC, whereas the values derived by XRD were smaller to those derived by DSC. The difference between the values is caused by the entirely different measuring principle of the two methods and the indefinite boundary between the crystalline and noncrystalline regions. Even so, the same variation trend of the crystallinity values allows the application of the two methods in crystallinity analysis.

To further analyze the effects of nano-TiO_2 on crystalline behavior of the composites, the crystal size of composites were calculated based on Scherrer equation as follows:

$$D = K\lambda / B\cos\ \theta \quad (6)$$

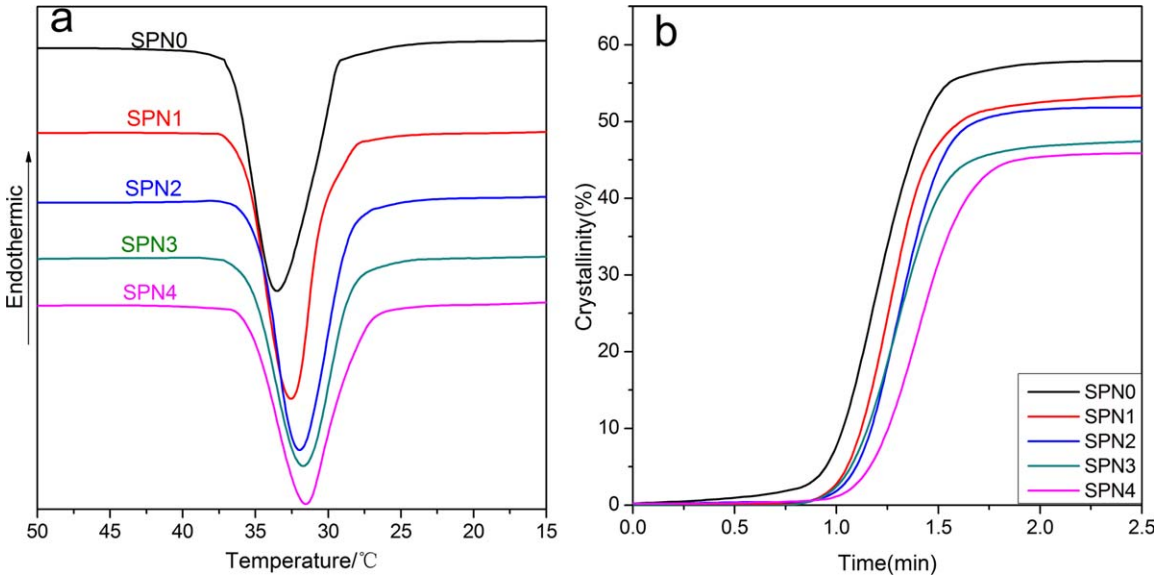

Figure 6. (a) DSC cooling thermograms and (b) plots of X_c versus time for the crystallization of SPN composites. [Color figure can be viewed in the online issue, which is available at wileyonlinelibrary.com.]

where D represents the average thickness of crystalline grain, which is vertical to the direction of the crystal face; K is Scherrer constant (taken to be 0.89); λ is the wavelength of X-ray (for Cu target, taken to be 1.54 Å); B is the half-height width of diffraction peak; θ is Bragg angle in degrees.

The results of the crystal size of composites were listed in Table I. It can be observed that the Bragg angle and crystal size of composites almost remained the same with the increasing of nano-TiO_2 content, which indicated that the crystal form and crystal size of PCL were unchanged. However, the formation of a interpenetrating network structure by combining nano-TiO_2 with starch/PCL prohibited the crystal grain from growing into a perfect lamellar structure during the cooling crystallization process.[38,39] As a result, the crystallinity degree of composites decreased with the increasing of nano-TiO_2 content.

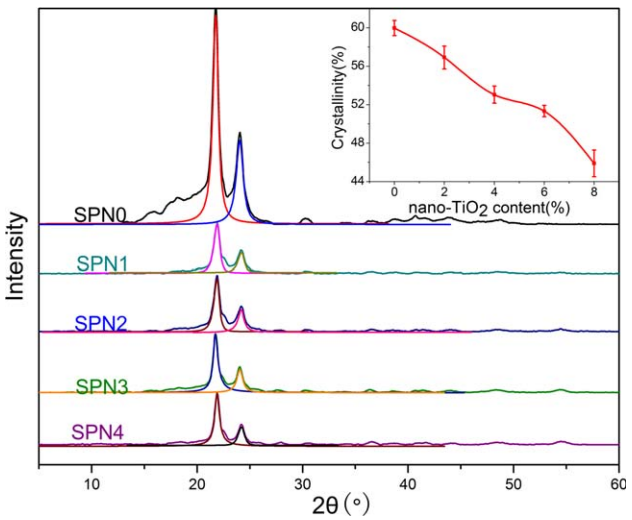

Figure 7. X-ray diffraction patters and the crystallinity degree of the composites with different contents of nano-TiO_2. The differences of crystallinity degree of SPN composites are significant ($P \leq 0.05$). [Color figure can be viewed in the online issue, which is available at wileyonlinelibrary.com.]

Mechanical Properties

The influence of nano-TiO_2 content on the bending strength and bending modulus of the blend composites was studied and the results were shown in Figure 8. When the nano-TiO_2 content in the composites increased from 0% to 6%, the bending strength and bending modulus of the composites increased by 60.8% and 64.1%, respectively. Interestingly, the crystallinity degree of the composites decreased. The crystallinity degree of the polymers had an important impact on their mechanical properties. In general, PCL was in a rubbery state at room temperature, and its bending strength and bending modulus decreased as the crystallinity degree decreases. But in this case, the intermolecular interfacial adhesion and the molecular chains rigidity of starch/PCL were enhanced with the existence of hydrogen and covalent bonds between nano-TiO_2 and starch/PCL, which greatly improved the bending strength and bending modulus of the composites and masked the influence of the crystallinity degree.

Meanwhile, the bending strength and bending modulus decreased slightly when the nano-TiO_2 content increased to 8%, which might be attributed to the destructive effects of excessive rigid nanoparticles on polymer structure.

Water Absorption and Water Solubility Investigation

In Figure 9, the water absorption of the composites slightly decreased with the addition of 2 wt % nano-TiO_2. Owing to the formation of hydrogen and covalent bonds between TiO_2 and starch/PCL, the free volume[25] of the composites decreased. The diffusion of water molecules in the composites was hindered, hence, the water absorption of the composite exhibited

Table I. X-ray Diffraction Data of the Samples

	2θ (deg)		B (rad)		D (nm)	
Samples	(110)	(200)	(110)	(200)	(110)	(200)
SPN0	21.870	24.128	1.167×10^{-2}	1.460×10^{-2}	11.959	9.603
SPN1	21.878	24.188	1.160×10^{-2}	1.458×10^{-2}	12.031	9.612
SPN2	21.913	24.181	1.162×10^{-2}	1.460×10^{-2}	12.018	9.602
SPN3	21.822	24.058	1.166×10^{-2}	1.458×10^{-2}	11.968	9.614
SPN4	21.885	24.213	1.166×10^{-2}	1.457×10^{-2}	11.973	9.620

the decreasing tendency. However, the water absorption of the SPN composites became higher when they contained more nano-TiO_2, because the abundant free hydroxyl groups and the high surface energy of nano-TiO_2 might be beneficial for adsorbing water. In addition, the microporous structure of the composites could enhance the water absorption ability. In Figure 9, the water solubility of the composites decreased with the increasing of nano-TiO_2. The water solubility of the SPN0 composite was 6.95%, whereas that of SPN3 was 4.16%. This was because the formation of a network structure between nano-TiO_2 and starch/PCL could enhance the interaction among the molecular chains, and further inhibited the scission of these chains in water solutions. Furthermore, the network structure restricted the motion of the low molecular weight polymer, monomer, and TiO_2, and reduced the mass loss of composites in water, so the water resistance of the composites improved. The water solubility of the composite slightly increased when nano-TiO_2 content reached 8 wt %, but it was still much lower than that of the SPN0 composites. The reason for the increase of the water solubility was also because of the agglomeration of nano-TiO_2 and the saturation of the reaction between excessive nano-TiO_2 and starch/PCL.

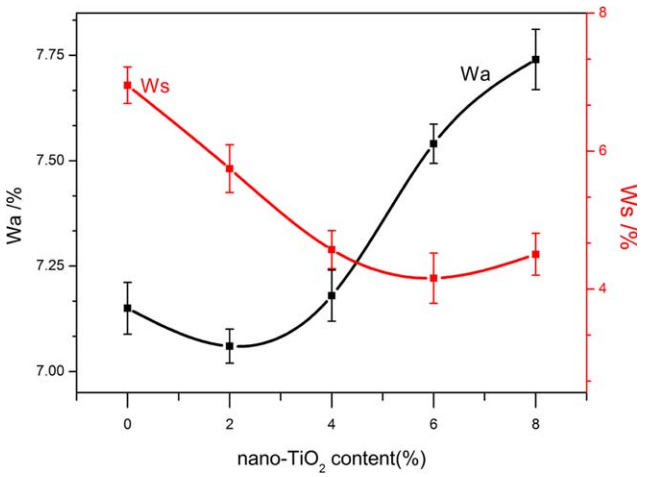

Figure 9. The dependence of the water absorption and water solubility on the nano-TiO_2 content of the SPN composites. The differences of water absorption and water solubility of two neighboring SPN composites are significant ($P \leq 0.05$). [Color figure can be viewed in the online issue, which is available at wileyonlinelibrary.com.]

Optical Transmittance of the Composites

In Figure 10, the overall transmittance of the sheets was low because the composite films were slightly thick. In terms of the variation tendency, the transmittance sharply declined when the content of the nano-TiO_2 rose. In general, the transparency of the composites increased with the increasing of crystallinity. But

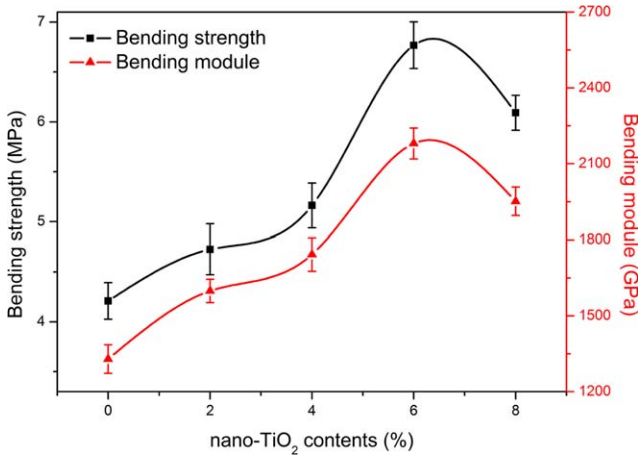

Figure 8. The bending strength and bending module of SPN composites. The differences of bending strength and bending module of SPN composites are significant ($P \leq 0.05$). [Color figure can be viewed in the online issue, which is available at wileyonlinelibrary.com.]

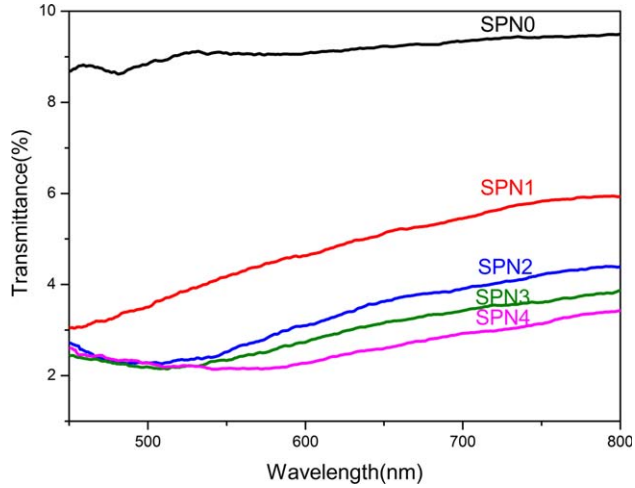

Figure 10. Transmittance of the SPN composites over a wavelength range of 450–800 nm. [Color figure can be viewed in the online issue, which is available at wileyonlinelibrary.com.]

in this case, because the diffuse reflection of light mainly occurred on the interface of the materials, the large specific surface-area and high refractive index of nano-TiO_2 greatly facilitated the diffuse reflection of light, consequently the transparency of the starch/PCL/nano-TiO_2 composites reduced.

CONCLUSIONS

In this study, the effects of nano-TiO_2 on the structure and properties of starch/PCL blend composites was investigated. The results demonstrated that the formation of hydrogen bonds and C-O-Ti bonds between nano-TiO_2 and polymer matrix generated an interpenetrating network structure, which greatly affected the characteristic of the starch/PCL composites. The crystallinity degree and crystallization rate of the composites decreased with the increasing of nano-TiO_2 content, whereas the crystal form and crystal size had no variation. The mechanical properties and water resistance of the composites improved significantly with the addition of nano-TiO_2. SPN3 exhibited the best bending strength and bending modulus, with the lowest water solubility. But for the high hydrophily of nano-TiO_2 and the improvement of the micropores structure of the composites, SPN1 had the lowest water absorption.

ACKNOWLEDGMENT

The authors gratefully acknowledge the financial assistance supported by "Twelfth Five-Year" National Science and Technology Support Program (NO. 2012BAD54G01), Huazhong Agricultural University Scientific & Technological Self-innovation Foundation (No. 2012SC21), National Natural Science Foundation of China (No. 20976066), Fundamental Research Funds for the Central Universities(No. 2011PY152).

REFERENCES

1. Kumar, M.; Mohanty, S.; Nayak, S. K.; Parvaiz, M. R. *Bioresour. Technol.* **2010**, *101*, 8406.
2. Orhan,Y.; Büyükgüngör, H. *Int. Biodeter. Biodegr.* **2000**, *45*, 49.
3. Flemming, H. C. *Polym. Degrad. Stabil.* **1998**, *59*, 309.
4. Ishiaku, U. S.; Pang, K. W.; Lee, W. S.; Ishak, Z. A. *Eur. Polym. J.* **2002**, *38*, 393.
5. Francesco, D. I.; Bellia, G.; Tosin, M.; Kapanen, A.; Itävaara, M. *Polym. Degrad. Stabil.* **2001**, *73*, 101.
6. Darwis, D.; Mitomo, H.; Yoshii, F. *Polym. Degrad. Stabil.* **1999**, *65*, 279.
7. Ahameda, N. T.; Singhala, R. S.; Kulkarnia, P. R.; Kalea, D. D.; Palb, M.; *Carbohydr. Polym.* **1996**, *31*, 157.
8. Matzinos, P.; Tserki, V.; Kontoyiannis, A.; Panayiotou, C. *Polym. Degrad. Stabil.* **2002**, *77*, 17.
9. Wang, L.; Ma, W.; Gross, R. A.; McCarthy, S. P. *Polym. Degrad. Stabil.* **1998**, *59*, 161.
10. Fujimaki, T. *Polym. Degrad. Stabil.* **1998**, *59*, 209.
11. Singh, R. P.; Pandey, J. K.; Rutot, D.; Degée, Ph.; Dubois, Ph. *Carbohydr. Res.* **2003**, *338*, 1759.
12. Li, S.; Tenon, M.; Garreau, H.; Braud, C.; Vert, M. *Polym. Degrad. Stabil.* **2000**, *67*, 85.
13. Hakkarainen, M. *Adv. Polym. Sci.* **2002**, *157*, 113.
14. Eldsäter, C.; Erlandsson, B.; Renstad, R.; Albertsson, A. C.; Karlsson, S. *Polymer*, **2000**, *41*, 1297.
15. Ohtaki, A.; Akakura, N.; Nakasaki, K. *Polym. Degrad. Stabil.* **1998**, *62*, 279.
16. Bastioli, C.; Cerutti, A.; Guanella, I.; Romano, G. C.; Tosin, M. *J. Environ. Polym. Degrad.* **1995**, *3*, 81.
17. Koenig, M. F.; Huang, S. *J. Polymer* **1995**, *9*, 1877.
18. Dubois, Ph.; Jacobs, C.; Jerome, R.; Teyssie, Ph. *Macromolecules* **1991**, *24*, 2266.
19. Spencer, M. W.; Cui, L. L.; Yoo, Y. J.; Paul, D. R. *Polymer* **2010**, *51*, 1056.
20. Wu, C. S. *Polym. Degrad. Stabil.* **2003**, *80*, 127.
21. Chen, L.; Zhang, Z.; Zhuang, X. L.; Chen, X. S.; Jing, X. B. *J. Appl. Polym. Sci.* **2010**, *117*, 2724.
22. Vertuccio, L.; Gorrasi, G.; Sorrentino, A.; Vittoria, V. *Carbohydr. Polym.* **2009**, *75*, 172.
23. Thipmanee, R.; Sane, A. *J. Appl. Polym. Sci.* **2012**, *126*, E252–E259.
24. Melhem, H.; Simon, P.; Wang, J; Bin, C. D.; Ratier, B.; Leconte, Y.; Herlin-Boime, N.; Makowska-Janusik, M.; Kassiba, A.; Bouclé, J. *Sol. Energ. Mat. Sol. C.*, in press. http://dx.doi.org/10.1016/j.solmat.2012.08.017.
25. Zhang, F. S.; Nriagu, J. O.; Itoh, H. *J. Photochem. Photobiol. A.* **2004**, *167*, 223.
26. Zhang, L.; Bai, X.; Tian, H.; Zhong, L. L.; Ma, C. L.; Zhou, Y. Z.; Chen, S. L.; Li, D. L. *Carbohydr. Polym.* **2011**, *89*, 1060.
27. Li, F.; Li, Q. M.; Kim, H. *Appl. Surf. Sci.* **2013**, *276*, 390.
28. Park, H. R.; Chough, S. H.; Yun, Y. H.; Yoon, S. D. *J. Polym. Environ.* **2005**, *13*, 375.
29. Liu, H. X.; Yuanyuan Huang, Y. Y.; Yuan, L.; He, P. S.; Cai, Z. H.; Shen, Y. L.; Xu, Y. M.; Yu, Y.; Xiong, H. G. *Carbohydr. Polym.* **2010**, *79*, 513.
30. Bagwasi, S.; Tian, B. Z.; Zhang J. L.; Nasir, M. *Chem. Eng. J.* **2013**, *217*, 108.
31. Kandel, D.; Kaxiras E. *Phys. Rev. Lett.* **1996**, *76*, 1114.
32. Nakata, K.; Fujishima, A. *J. Photochem. Photobiol. C.* **2012**, *13*, 169.
33. Tochihara, H.; Shirasawa, T. *Prog. Surf. Sci.* **2011**, *86*, 295.
34. Li, Y.; Sasaki, T.; Shimizu, Y.; Koshizaki N. *Small* **2008**, *4*, 2286.
35. Miao, Z. J.; Ding, K. L.; Wu, T. B.; Liu, Z. M.; Han, B. X.; An, G. M.; Miao, S.; Yang, G. Y. *Micropor. Mesopor. Mater.* **2008**, *111*, 104.
36. Crescenzi, V.; Manzini, G.; Calzolari, G.; Borri, C. *Eur. Polym. J.* **1972**, *8*, 449.
37. Cong, P. H.; Xiang, F.; Liu, X. J.; Li, T. S. *Wear* **2008**, *265*, 1106.
38. Chiu, F. C.; Yen, H. Z.; Lee, C. E. *Polym. Test.* **2010**, *29*, 397.
39. Lee, S. Y.; Park, S. Y.; Song, H. S. *Polymer* **2006**, *47*, 3540.